

Dipolar Interaction and Sample Shape Effects on the Hysteresis Properties of $2d$ Array of Magnetic Nanoparticles

Manish Anand*

*Department of Physics, Bihar National College,
Patna University, Patna-800004, India.*

(Dated: October 26, 2021)

Abstract

We study the ground state and magnetic hysteresis properties of $2d$ arrays ($L_x \times L_y$) of dipolar interacting magnetic nanoparticles (MNPs) by performing micromagnetic simulations. Our primary interest is to understand the effect of sample shape, Θ - the ratio of the dipolar strength to the anisotropy strength, and the direction of the applied field $\vec{H} = H_o \hat{e}_H$ on the ground state and the magnetic hysteresis in an array of MNPs. To study the effect of shape of the sample, we have varied the aspect ratio $A_r = L_y/L_x$ which in turn, is found to induce shape anisotropy in the system. Our main observations are: (a) When the dipolar interaction is strong ($\Theta > 1$), the ground state morphology has in-plane ordering of magnetic moments. (b) The ground state morphology has randomly oriented magnetic moments which is robust with respect to system sizes and A_r for weakly interacting MNPs ($\Theta < 1$). (c) Micromagnetic simulations suggests that the dipolar interaction decreases the coercive field H_c . (d) The remanence magnetization M_r is found to be strongly dependent not only on the strength of dipolar interaction but also on the shape of the sample. (e) Due to anisotropic nature of dipolar interaction, a strong effect of shape anisotropy is observed when the field is applied along longer axis of the sample. The dipolar interaction in such a case induces an effective ferromagnetic coupling when the aspect ratio is very large. These results are of vital importance in high-density recording systems, magneto-impedance sensors, etc.

* itsanand121@gmail.com

I. INTRODUCTION

Magnetic nanoparticles (MNPs) arrays are of profound importance not only because of interesting physics but also due to their numerous technological applications [1–12]. For instance, a two-dimensional array of MNPs is a suitable system for high-density digital storage and perpendicular recording media [13–15]. The magnetic properties in such a case depend strongly on the shape, size, geometry of the systems and the magnetic interactions. The primary magnetic interaction in such systems is dipole-dipole interactions. The dipolar interaction is long-ranged and favours ferromagnetic as well as antiferromagnetic coupling. As a result, unconventional morphologies are observed when the size of the system is comparable to the range of dipolar interactions. Due to anisotropic nature of dipolar interactions, there have also been observations of ferromagnetic, striped, checkerboard patterns, vortices, etc. depending on the geometry of the lattice [16–21]. The magnetic hysteresis properties in such systems are found to be greatly influenced by the dipolar interactions [22–25]

There are several studies in the literature which make an implicit and explicit reference to the ubiquitous dipolar interactions and anisotropy in ordered arrays of MNPs. We summarize below few of them which is relevant to our present work: (a) Li *et al.* studied the ground state, magnetic specific and magnetic hysteresis properties for three types of closely spaced nanomagnet arrays using Monte Carlo simulation [26]. They observed vortex state due to the dipolar interactions in these arrays. For face-centred cubic nanomagnet arrays, a slight jump occurs in the hysteresis curve. (b) Using the micromagnetic simulation, Yang *et al.* studied the magnetic properties in two-dimensional arrays of MNPs [27]. They found that coercivity increases with arrays disorder. (c) Using the Landau-Lifshitz-Gilbert approach, Morales-Meza *et al.* studied the magnetization reversal in a two-dimensional array of MNPs [28]. They showed that coercivity is reduced even if the particle position in the array is random. (d) Chinni *et al.* performed experiments and micromagnetic simulation using Object Oriented MicroMagnetic Framework (OOMMF) to study magnetic properties in nanocomposite films [29]. They observed an unexpected hysteretic behaviour characterized by in-plane anisotropy and crossed branches in the hysteresis curves measured along the hard direction. (e) Faure *et al.* studied the magnetic properties of ordered arrays of MNPs using experiment and Monte Carlo simulation [30]. The dipolar interaction is found to induce a ferromagnetic coupling that increases in strength with decreasing thickness of

the array. (f) Using theoretical calculations, Xue *et al.* studied the magnetic hysteresis properties of the two-dimensional hexagonal array of MNPs [15]. The hysteresis curves are found to vary their shapes from a rectangle to a non-hysteresis straight line through a set of complicated loops, in accordance with the magnetization reversal process.

Although the above studies imply that dipolar interaction and geometrical arrangement of MNPs affect the magnetic properties of an ordered array of MNPs, a systematic study as a function of dipolar interaction strength, shape anisotropy of the system and direction of the applied field is still missing. In this work, we attempt to understand the effect of dipolar interaction manipulated by changing the interparticle separation, the direction of applied magnetic field and shape anisotropy induced by varying the aspect ratio on the magnetic properties of two dimensional ($2d$) arrays of MNPs. The main questions which we have attempted to address are : (1) What are the consequences of dipolar interaction on ground state organizations of MNPs? (2) How are the magnetic hysteresis properties modified due to the dipolar interactions, shape anisotropy of the sample and direction of the applied magnetic field? To answer these questions, we consider $2d$ ($L_x \times L_y$) arrays of cubical shaped Fe_3O_4 MNPs. It is well known fact that uniformly magnetized cubical MNPs do not possess shape anisotropy [31]. But we have been able to induce it in the system by just varying the sample shape. It will be shown that the latter has a drastic effect on the hysteresis behaviour. These ordered arrays of MNPs have many interesting properties due to structural order, well defined interparticle interactions and geometry confinement [32]. In such a case, MNPs are coated with an inorganic surfactant to prevent agglomeration during self-assembling. Due to this MNPs are at a well distance beyond the range of exchange interaction. As a consequence, the predominant interaction in such arrays is dipolar interaction [33]. The energy of such an assembly is, therefore, given by the sum of the anisotropy energy and the dipolar interaction energy.

To vary the relative dipolar interaction strength with respect to anisotropy strength, we have defined a ratio $\Theta = D/KV$ where D is the strength of dipolar interaction, K is the anisotropy constant, and V is the volume of the nanoparticle. The value of Θ for various interparticle separation a for Fe_3O_4 has been given in Table I. We refer to $\Theta > 1$ as the strong dipolar interaction regime, $\Theta < 1$ as the weak dipolar interaction regime. We have performed micromagnetic simulation using OOMMF code from NIST [34]. In OOMMF code, the finite difference method is employed, which requires discretization of a chosen geometry over a

grid of identical prism-cells, and the magnetization is supposed to be uniform in each cell. In the implementation of OOMMF, the continuous magnetic material is divided in discrete cubes (i.e. grid cells), which are in geometrical contact. This discretization scheme suits to a continuous magnetic film rather than an assembly of non-touching nanoparticles. Due to this reason, this type of modelling does not discriminate between the magnetic behavior of $2d$ continuous films and $2d$ nanoparticle arrays. To overcome this, we have put exchange interaction to zero to mimic the separated MNPs arrays magnetically. The absence of exchange interaction is also needed for the MNPs where they are coated with a surfactant to avoid agglomeration. We have successfully implemented it in our earlier studies [35, 36]. We have used Landau-Lifshitz-Gilbert (LLG) equation which is used to describe the precessional motion of a moment in magnetic field at $T = 0$ K. We have solved the coupled equation of motion for the given lattice to obtain the minimum energy configurations. To study the hysteresis, we have applied a dc magnetic field $\mu_o\vec{H} = H_o\hat{e}_H$, where $\hat{e}_H = \hat{x}$, \hat{y} and \hat{z} is the direction of the applied field along x , y and z -axis respectively. We also study the role of aspect ratio $A_r = L_y/L_x$ to induce shape anisotropy in the system and the direction of the field \hat{e}_H .

The interplay of anisotropy, dipolar energy and aspect ratio creates unusual morphologies which have profound implications on the magnetic properties. Our work, therefore, throws light on this subject from a microscopic picture and provides a basis for results obtained in experimental and theoretical studies. This paper is organized as follows. In Section II, we introduce the model for an array of MNPs, the LLG equation, which provides the prototypical ground state (GS) morphologies and equilibrium morphologies. In Sec. III, we present our numerical results and discuss the dependence of the magnetic hysteresis on Θ , aspect ratio $A_r = L_y/L_x$ and the direction of the applied field \hat{e}_H . A conclusion of our results is provided in Section IV.

II. MODEL AND METHODOLOGY

A. Model for Dipolar Interacting Arrays of MNPs

We consider a self-assembled $2d$ array ($L_x \times L_y$) of cubical shaped magnetic nanoparticles in the xy -plane. The total number of the MNPs in the assembly are $N = L_x/a \times L_y/a$,

where l is the length of an edge of the particle and a is the lattice spacing. Each MNP has magnetic moment $\vec{\mu}_i = \mu \hat{e}_i$, $i = 1, 2, \dots, N$. The magnitude of the magnetic moment $\mu = M_s V$ where M_s is the saturation magnetization and $V = l^3$ is the volume of the magnetic nanoparticle. The MNPs are assumed to have uniaxial anisotropy $\vec{K} = K \hat{k}_i$ where K is the anisotropy constant, and \hat{k}_i is the direction of the anisotropy. Generally, MNPs are coated with a surfactant to prevent agglomeration, which suppresses the exchange interactions. The energy of such a system, therefore, includes contribution from anisotropy energy E_a and dipolar interaction E_d [37, 38]:

$$E = E_a + E_d = -KV \sum_i (\hat{k}_i \cdot \hat{e}_i)^2 - D \sum_{i,j} \frac{3(\hat{e}_i \cdot \hat{r}_{ij})(\hat{e}_j \cdot \hat{r}_{ij}) - (\hat{e}_i \cdot \hat{e}_j)}{(r_{ij}/a)^3}, \quad (1)$$

where μ_o is the permeability of free space, \hat{e}_i is the unit vector along the magnetic moment, r_{ij} is the distance between particles i and j , and \hat{r}_{ij} is the unit vector along with it. The $1/r_{ij}^3$ dependence means that the dipolar interaction is long ranged in nature. The analytical calculation of dipolar interaction between cubical shaped MNPs can be found in the reference [39]. It is well known fact that self assembled MNPs usually form $2d$ close-packed hexagonal lattices but magnetic properties are found to be nearly independent of the structure of the lattice [40].

Here we define the *dipolar interaction strength* $D = \mu_o \mu^2 / 4\pi a^3$. As magnetic properties of such an assembly are governed by the relative strength of the anisotropy and dipolar energy, we have defined a ratio $\Theta = D/KV$. Although dipolar interactions and anisotropy energy depend on various system parameters, the behaviour of the assembly will be dictated by Θ rather than the precise values of parameters such as a , V , μ and K . When D is greater than KV , the dipolar interaction is stronger than anisotropy i.e $\Theta > 1$. Similarly, $\Theta < 1$ can be termed as the weak dipolar regime.

In the presence of an external magnetic field $\mu_o \vec{H}$, there is an additional contribution to energy E given by [38]

$$E_H = -H_o \sum_{i=1} \vec{\mu}_i \cdot \hat{e}_H, \quad (2)$$

here H_o is the magnitude of field and \hat{e}_H is the unit vector in the direction of applied field.

B. Landau-Lifshitz-Gilbert Equation

The precessional motion of the magnetic moment $\vec{\mu}_i$ in a magnetic field can be described by the LLG equation [41]:

$$\frac{d\vec{\mu}_i}{dt} = -\gamma\vec{\mu}_i \times \vec{H}_i^e - \lambda\vec{\mu}_i \times (\vec{\mu}_i \times \vec{H}_i^e), \quad i = 1, 2, \dots, N, \quad (3)$$

where γ is the electron gyromagnetic ratio, $\lambda = \gamma\alpha/M_s$ is a phenomenological dimensionless damping factor, and $\vec{H}_i^e = -\partial E_T/\partial\vec{\mu}_i$ is the effective field experienced by magnetic moment, where $E_T = E + E_H$. While studying ground state properties, E_H is taken to be zero. The first term in Eq. (3) takes care of the precession of $\vec{\mu}_i$ around \vec{H}_i^e . The second term is due to a phenomenological dissipative motion: the magnetic moment $\vec{\mu}_i$ precesses around \vec{H}_i^e . The solution of these coupled differential equations yields the GS configuration $\{\vec{\mu}_i\}$, of the assembly.

To perform micromagnetic simulation using OOMMF code, the entire system is discretized into cells where each has lateral dimension l say. Each cell in such case represents a magnetic moment $\mu = M_s V$. The centre-to-centre separation between moments is, therefore, $l \equiv a_0$. By our formulation in Eq. (1), the strength of the dipolar interaction can be manipulated by varying the centre-to-centre separation a of the MNPs. However, with the protocol implemented in OOMMF, a change in the centre-to-centre separation from a_0 to a_β say, changes the cell volume from $V \equiv V_0 (= a_0^3)$ to $V_\beta (= a_\beta^3)$. As a consequence, the magnetic moment gets altered to $\mu_\beta = M_s V_\beta$, which ultimately modifies the magnetic properties of the particles under study. This undesirable artefact in the simulation needs to be overcome. To overcome this artefact, we formulated a rescaling method for saturation magnetization:

$$M_s^\beta = M_s^0 \frac{V_0}{V_\beta}, \quad (4)$$

where M_s^0 is the saturation magnetization for nano particle of volume $V_0 = a_0^3$. It is easy to see that now $\mu = M_s^0 V_0 = M_s^\beta V_\beta$ as desired. Corresponding changes need to be incorporated in other related variables of interest such as the coercive field H_c and the anisotropy field $H_K = 2K/M_s$ [42] for non-interacting or weakly interacting MNPs which play an important

role in hysteresis:

$$H_c^\beta = H_c^0 \frac{V_\beta}{V_0}, \quad (5)$$

$$H_K^\beta = H_K^0 \frac{V_\beta}{V_0}. \quad (6)$$

We have successfully implemented this scaling procedure to study the heat dissipation and spin transport properties in the assembly of dipolar interacting MNPs in our earlier work [35, 36].

III. NUMERICAL RESULTS

We consider cubical shaped MNPs of Fe_3O_4 arranged on a $2d$ ($L_x \times L_y$) lattice. The particle size is chosen to be $l = 10$ nm. We have used anisotropy constant $K = 13 \times 10^3$ Jm⁻³ and saturation magnetization $M_s = 4.77 \times 10^5$ A/m for numerical evaluations. The six values of interparticle separation a are considered for magnetic hysteresis study: $a_0 = 10$ nm, $a_1 = 12$ nm, $a_2 = 16$ nm, $a_3 = 20$ nm, $a_4 = 30$ nm and $a_5 = 40$ nm. Table I provides the values of Θ for these interparticle separations. The initial condition that we choose for the assembly of MNPs is random orientations of magnetic moments and anisotropy axes. All the data obtained using the simulations are averaged over 50 sets of initial conditions. The ground state morphologies are obtained by solving LLG equation using OOMMF code in the absence of external magnetic field. To study the magnetic hysteresis properties, we apply a dc magnetic field of strength -150 mT to 150 mT for $a = 10$ nm. For other interparticle separations, the scaled saturation magnetization M_s^β were obtained using Eq. (4). The corresponding H_c^β and H_K^β were calculated using Eqs. (5) and (6), respectively. We have chosen the magnetic field to be large enough as compared to H_c to achieve saturation and the ramping up or slowing down has been appropriately fine-tuned to capture the magnetic properties near H_c . We study the dependence of magnetic hysteresis on the Θ , aspect ratio $A_r = L_y/L_x$ and the direction of the applied field \hat{e}_H . In our simulations, $L_x = 120$ nm; $A_r = 1, 2, 4, 8, 16$ and 32 ; $\Theta = 1.75, 1.01, 0.42, 0.22, 0.06$ and 0.03 ; $\hat{e}_H = \hat{x}, \hat{y}$ and \hat{z} .

A. Ground State (GS) Morphologies

We first study the effect of Θ and A_r on ground state spin morphologies. For this purpose, we look square samples i.e $A_r = 1.0$ such that $L_x \times L_y \equiv L_x \times L_x$. Fig. (1) depicts GS morphologies for $L_x = 120$ nm. The interparticle separation a is chosen to be 10 nm [see Fig. 1(a)] and 20 nm [see Fig. 1(b)]. These correspond to $\Theta = 1.75$ and 0.22, respectively. So the number of spins in Fig. 1(a) is 12×12 and 6×6 in Fig. 1(b). we depict the spins with non-zero z -component by the green cone. Those lying in the xy plane with a positive x -component have been indicated by the red coloured cone, while those with negative x -component by the blue coloured cone. It is quite evident that for strongly interacting MNPs ($\Theta = 1.75$), *all* the spins are in the xy -plane [see Fig. 1(a)]. They exhibit locally ordered regions. On the other hand, when magnetic interactions are weak ($\Theta = 0.22$), the moments are randomly oriented, signifying lack of magnetic order [see Fig. 1(b)]. Magnetic moments also tend to align normal to the plane of the sample. It means that dipolar interaction favours in-plane ordering. Then, we study the effect of aspect ratio A_r on the spin morphologies. For $\Theta < 1$, the features are unchanged as A_r is increased to 2, 3, 4, etc. and are prototypically represented by Fig. 1(b). We do not show them to avoid repetition. In Fig. (2), we depict morphologies corresponding to the strongly dipolar interacting MNPs ($a = 10$ nm, $\Theta = 1.75$) for $L_x = 120$ nm and two aspect ratio (a) $A_r = 2$ [see Fig. 2(a)] and (b) $A_r = 4$ [see Fig. 2(b)]. In both the cases, the MNPs exhibit local order and prefer to lie in the xy -plane. The morphology of the magnetic moments near the sample edges is very distinct from that in the bulk. The moments tend to align along the edges as ferromagnetic chains.

B. Magnetic Hysteresis Study

Next, we study the effect of dipolar strength Θ , shape anisotropy of the sample and direction of applied field \hat{e}_H on the magnetic hysteresis in a systematic manner. To vary the dipolar interaction strength, we have varied the interparticle separation. To induce shape anisotropy in the system, we have changed the aspect ratio A_r of the sample. In Fig. (3), we have plotted magnetic hysteresis curves for square sample, i.e., $L_x = L_y = 1.0$ as a function of Θ and \hat{e}_H . We have considered six values of dipolar strength $\Theta = 1.75, 1.01, 0.42, 0.22,$

0.06 and 0.03 in each case. The magnetic field axis (x -axis) has been scaled by H_K , the anisotropy field (for non-interacting MNPs with randomly oriented anisotropy axes). The direction of the external field is (a) $\mu_o\vec{H} = H_o\hat{x}$ [see Fig. 3(a)], (b) $\mu_o\vec{H} = H_o\hat{y}$ [see Fig. 3(b)] and (c) $\mu_o\vec{H} = H_o\hat{z}$ [see Fig. 3(c)]. It is quite evident that when the field is applied in the plane of the sample, i.e., either along x or y -direction, the coercive field H_c decreases with an increase in the strength of dipolar interaction. As a consequence, the area under the hysteresis curve diminishes. When the field is applied normal to the plane of the sample (z -direction), magnetic moment ceases to follow the applied field for $\Theta > 1$. As a result, non-hysteresis is observed, so H_c and M_r tend to zero for strongly interacting MNPs. It is clearly seen that the coercive field $H_c \approx 0.48H_K$ and $M_r \approx 0.5$ for weak interaction or non-interacting MNPs ($\Theta < 1$) irrespective of the direction of the applied field. These values of H_c and M_r correspond to single particle hysteresis with randomly oriented anisotropy axis [42, 43]. It means that magnetic hysteresis follows the Stoner-Wohlfarth model when the interaction among the MNPs is weak as expected [42, 43].

To study the dependence of shape anisotropy on the magnetic properties, we study the magnetic hysteresis as a function of aspect ratio A_r for various values of Θ and three directions of the applied field, i.e., along x , y and z -axis respectively. We have considered six values of aspect ratio $A_r = 1.0, 2.0, 4.0, 8.0, 16.0$ and 32.0 in each case. In Fig. (4), the direction of the applied field is in the plane of the sample [$\mu_o\vec{H} = H_o\hat{x}$ and $\mu_o\vec{H} = H_o\hat{y}$]. The values of Θ are (a) $\Theta = 1.75$ [see Fig. 4(a) and 4(e)], (b) $\Theta = 1.01$ [see Fig. 4(b) and 4(f)], (c) $\Theta = 0.42$ [see Fig. 4(c) and 4(g)] and (d) $\Theta = 0.22$ [see Fig. 4(d) and 4(h)]. The direction of the applied field is normal to the plane of the sample (along the z -axis) in Fig. (5). The other parameters, A_r and Θ in Fig. (5) remain the same as that of Fig. (4). When the applied field is along the shorter axis (along the x -axis), dipolar interaction decreases the value of H_c and M_r [see Fig. 4(a)-(d)]. There is a weak dependence of H_c on A_r . For weakly interacting MNPs, hysteresis curves follow the Stoner-Wohlfarth model [43]. A strong effect of shape anisotropy is observed when the field is applied along the increasing length of the sample, i.e., along the y -axis. The remanent magnetization M_r increases with increase in A_r , and it reaches to 0.9 for strongly interacting MNPs [see Fig. 4(e)]. In this case, also, the larger is the strength of dipolar interaction, the smaller is the value of H_c [see Fig. 4 (e)-(h)]. The magnetic moments cease to follow the applied magnetic field when the field is applied along the z -axis for strongly interacting MNPs. As a consequence, almost no hysteresis is

observed for strongly interacting MNPs with applied field normal to the plane of the sample [see Fig. 5(a)-(b)]. Like the other two cases stated above, weakly interacting MNPs follow the Stoner-Wohlfarth model irrespective of A_r .

C. Characterization of Magnetic Hysteresis Curves

Finally, we study the variation of the coercive field H_c and M_r as a function of Θ , A_r and \hat{e}_H by extracting their values from the simulated magnetic hysteresis curves. In Fig. (6), we have plotted variation of H_c (scaled by H_K) and M_r as function of dipolar strength Θ for six values of aspect ratio $A_r = 1.0, 2.0, 4.0, 8.0, 16.0$ and 32.0 . The direction of the applied magnetic field is (a) $\mu_o\vec{H} = H_o\hat{x}$ [see Fig. 6(a) and 6(d)], (b) $\mu_o\vec{H} = H_o\hat{y}$ [see Fig. 6(b) and 6(e)] and (c) $\mu_o\vec{H} = H_o\hat{z}$ [see Fig. 6(c) and 6(f)]. With the field applied along the x -axis, H_c decreases with an increase in the strength of dipolar interaction Θ and its value drops to $0.1H_K$ for $A_r = 32.0$ and $\Theta = 1.75$ [see Fig. 6(a)]. The variation of H_c is similar as with field along x -axis when the field is applied longer axis of the sample (along the y -axis), but the value of H_c is slightly higher in this case for $A_r = 32.0$ and $\Theta = 1.75$ [see Fig. 6(b)]. When the field is applied normal to the plane of the sample, H_c decreases very fast with an increase in Θ and A_r . Its value drops down to zero for strongly interacting MNPs, and $A_r = 32.0$ [see Fig. 6(c)]. There is a weak dependence of M_r on A_r when the field is applied along the x -axis [see Fig. 6(d)]. There is a strong effect of shape anisotropy when the field is applied along y -axis [see Fig. 6(e)]. For strongly interacting MNPs, M_r increases as the aspect ratio A_r is increased and it reaches to 0.9 for $\Theta = 1.75$, and $A_r = 32.0$ [see Fig. 6(e)]. M_r decreases very sharply with Θ , and its value drops to zero for $\Theta = 1.75$ when the magnetic field is applied normal to the plane of the sample [see Fig. 6(f)]. For weakly interacting MNPs, magnetic hysteresis curves follow the Stoner-Wohlfarth model irrespective of aspect ratio and direction of the applied field, which is reflected in H_c ($\approx 0.48H_K$) and M_r (≈ 0.5).

These results can be explained by probing the effect of dipolar interaction and shape anisotropy of the sample induced by varying aspect ratio. It is evident from the ground state morphologies that the dipolar interactions favour in-plane ordering of magnetic moments. When A_r is increased, the dipolar interaction favours ferromagnetic coupling between the magnetic moments. It is because of the fact the demagnetization field decreases as shape anisotropy is increased (A_r increases in our case), which is also reported by Wysin [44]. As a

consequence, magnetic moments tend to align along the longer axis of the sample as it costs less energy as compared to other configurations. It has also been reported by Jordanovic *et al.* [9]. This ferromagnetic coupling for strongly interacting MNPs can also be explained by that fact that the exchange interaction between the MNPs is assumed to be zero in the present work. Due to the absence of exchange interaction, the energetics of domain walls are entirely controlled by the dipolar interaction. It makes energetically favourable to form domain walls along the increasing length of the sample. When an external field is applied to these systems system, the response of this system not only depends on the dipolar strength but also on the shape anisotropy of the sample which has been induced by increasing A_r in our work. When the field is applied along the shorter axis of the sample, i.e., along the x -axis, the natural tendency to get aligned along the longer axis of the sample is hindered. As a result, magnetic moment ceases to follow the external field, which is reflected in a decrease in the value of M_r (≈ 0.1) and H_c to $0.1H_K$ for strongly interacting MNPs with $A_r = 32.0$. Magnetic moments are found to follow the field when the field is applied along the longer axis of the sample, but due to the increase in the strength of dipolar interaction as well, H_c decreases, but its value remains slightly higher as that of the previous situation. Due to the same reason, M_r increases with A_r for $\Theta > 1$. This increase of M_r and decrease of H_c when the field is applied along the longer axis of the sample is in qualitative agreement with the work done by García-Arribas *et al.* [45]. They have studied the shape anisotropy effect in a thin film permalloy microstrips.

When we force the magnetic moments to get aligned normal to the plane of the sample by applying the field along the z -axis, they oppose strongly for a large value of Θ and A_r . This happens due to the fact that the natural tendency of the magnetic moments is to get organized in the plane of the sample (xy -plane in our case). As a result, non-hysteresis is observed in this case, which is reflected in zero value of H_c and M_r . This non-hysteresis behaviour has also been reported by Xue *et al.* [15]. They have studied the hysteresis properties in a two-dimensional hexagonal array with aligned uniaxial anisotropy. From all the cases, it is quite evident that dipolar interaction always decreases the value of coercive field H_c . It is because of that dipolar interactions cause a collective reversal of the magnetic moments under an applied magnetic field and as a consequence, the coercive field decreases with an increase in dipolar interaction strength.

IV. CONCLUSION

To conclude, we have studied the effect of dipolar interactions and shape of the sample on the magnetic properties of $2d$ ($L_x \times L_y$) array of cubical shaped magnetic nanoparticles (MNPs) by performing micromagnetic simulation using OOMMF code [34]. It is well known that uniformly magnetized cubical shaped particles do not possess shape anisotropy [31] but we have been able to induce the latter in the system by varying aspect ratio A_r . Our primary aim was to study ground state (GS) morphologies, and understand the magnetic hysteresis properties as a function of Θ , shape anisotropy induced by varying the aspect ratio $A_r (= L_y/L_x)$ and the direction of the applied field $\mu_o \vec{H} = H_o \hat{e}_H$. Our observations are as follows: (a) For weakly interacting MNPs ($\Theta < 1$), the magnetic moments are randomly oriented, and the morphology is unaffected by A_r . MNPs also tend to align normal to the plane of the sample. (b) For strong dipolar strengths ($\Theta > 1$), magnetic moments prefer to orient in the plane of the sample. The morphology, in this case, comprises regions of correlated moments. (c) Magnetic moment favours ferromagnetic coupling along the longer axis of the sample when A_r is increased provided $\Theta > 1$. (d) When the dipolar interaction is weak; magnetic hysteresis curves follow the Stoner-Wohlfarth model ($H_c \approx 0.48H_K$ and $M_r \approx 0.5$) irrespective of the direction of applied field \hat{e}_H and aspect ratio A_r . (e) A strong effect of shape anisotropy is observed when the field is applied along the increasing length of the sample, which is reflected in the very large value of remanent magnetization $M_r \approx 0.9$. (f) The dipolar interaction always decreases the coercive field H_c . (g) For strongly interacting MNPs, H_c and M_r tend to zero when the field is applied normal to the plane of the sample.

We have succeeded in obtaining well guidelines regarding how magnetic hysteresis properties may change in the dipolar interacting MNPs arrays. The obtained results contribute to expanding the fundamental comprehension of two-dimensional dipolar interacting system and offer exciting implications for the creation of self-assembled arrays of magnetic nanoparticles of desired magnetic response. The micromagnetic simulation showed that the dipolar interaction induces an effective ferromagnetic coupling in thin arrays (when the aspect ratio is very large). It means that one can modulate the magnetic properties of the ordered arrays of MNPs by varying the strength of shape anisotropy of the system. The latter can be changed by varying the width and length of the system. Our results are also relevant for the experimental samples, which can be divided into various categories depending on how

they behave when an external magnetic field is applied to them.

ACKNOWLEDGMENTS

Most of the numerical simulations presented in this work have been carried out in the Department of Physics, Indian Institute of Technology (IIT) Delhi. I am grateful to Prof. Varsha Banerjee for providing the computational facility at IIT Delhi.

-
- [1] L. Wu, A. Mendoza-Garcia, Q. Li, and S. Sun, *Chemical reviews* **116**, 10473 (2016).
 - [2] K. Ulbrich, K. Hola, V. Subr, A. Bakandritsos, J. Tucek, and R. Zboril, *Chemical reviews* **116**, 5338 (2016).
 - [3] A. Hervault and N. T. K. Thanh, *Nanoscale* **6**, 11553 (2014).
 - [4] R. Bustamante, A. Millán, R. Piñol, F. Palacio, J. Carrey, M. Respaud, R. Fernandez-Pacheco, and N. J. O. Silva, *Physical Review B* **88**, 184406 (2013).
 - [5] C. A. Schütz, L. Juillerat-Jeanneret, H. Mueller, I. Lynch, and M. Riediker, *Nanomedicine* **8**, 449 (2013).
 - [6] J.-L. Déjardin, A. Franco, F. Vernay, and H. Kachkachi, *Physical Review B* **97**, 224407 (2018).
 - [7] P. Capiod, L. Bardotti, A. Tamion, O. Boisron, C. Albin, V. Dupuis, G. Renaud, P. Ohresser, and F. Tournus, *Physical Review Letters* **122**, 106802 (2019).
 - [8] V. F. Puentes and K. M. Krishnan, *IEEE transactions on magnetics* **37**, 2210 (2001).
 - [9] J. Jordanovic, M. Beleggia, J. Schiøtz, and C. Frandsen, *Journal of Applied Physics* **118**, 043901 (2015).
 - [10] Z. Zhong, B. Gates, Y. Xia, and D. Qin, *Langmuir* **16**, 10369 (2000).
 - [11] R. Cowburn, A. Adeyeye, and M. Welland, *New Journal of Physics* **1**, 16 (1999).
 - [12] M. Anand, *Journal of Magnetism and Magnetic Materials* **522**, 167538 (2021).
 - [13] M. Pardavi-Horvath, *Journal of magnetism and magnetic materials* **177**, 213 (1998).
 - [14] A. Mohtasebzadeh, L. Ye, and T. Crawford, *International journal of molecular sciences* **16**, 19769 (2015).
 - [15] D. Xue and Z. Yan, *Journal of applied physics* **100**, 103906 (2006).
 - [16] U. Löw, V. Emery, K. Fabricius, and S. Kivelson, *Physical Review Letters* **72**, 1918 (1994).

- [17] K. De'Bell, A. MacIsaac, I. Booth, and J. Whitehead, *Physical Review B* **55**, 15108 (1997).
- [18] E. Edlund and M. N. Jacobi, *Physical review letters* **105**, 137203 (2010).
- [19] M. Anand, V. Banerjee, and J. Carrey, *Physical Review B* **99**, 024402 (2019).
- [20] A. P. Alivisatos, *science* **271**, 933 (1996).
- [21] C. Collier, R. Saykally, J. Shiang, S. Henrichs, and J. Heath, *Science* **277**, 1978 (1997).
- [22] D. Kechrakos and K. Trohidou, *Physical Review B* **71**, 054416 (2005).
- [23] N. Usov, O. Serebryakova, and V. Tarasov, *Nanoscale research letters* **12**, 489 (2017).
- [24] L. C. Branquinho, M. S. Carrião, A. S. Costa, N. Zufelato, M. H. Sousa, R. Miotto, R. Ivkov, and A. F. Bakuzis, *Scientific reports* **3**, 2887 (2013).
- [25] M. Anand, *Journal of Applied Physics* **128**, 023903 (2020).
- [26] Y. Li, T. Wang, H. Liu, f. Dai, X. Yu, and G. Liu, *Journal of Nanomaterials* **16**, 331 (2015).
- [27] B. Yang and Y. Zhao, *Journal of Applied Physics* **110**, 103908 (2011).
- [28] M. Morales-Meza, P. P. Horley, A. Sukhov, and J. Berakdar, *The European Physical Journal B* **87**, 186 (2014).
- [29] F. Chinni, F. Spizzo, F. Montoncello, V. Mattarello, C. Maurizio, G. Mattei, and L. D. Bianco, *Materials* **10**, 717 (2017).
- [30] B. Faure *et al.*, *Nanoscale* **5**, 953 (2013).
- [31] R. Moskowitz and E. Della Torre, *IEEE Transactions on Magnetics* **2**, 739 (1966).
- [32] G. Held, G. Grinstein, H. Doyle, S. Sun, and C. Murray, *Physical Review B* **64**, 012408 (2001).
- [33] D. Kechrakos and K. Trohidou, *Journal of nanoscience and nanotechnology* **8**, 2929 (2008).
- [34] M. J. Donahue and D. G. Porter, National Institute of Standards and Technology, Gaithersburg, MD (1999).
- [35] M. Anand, J. Carrey, and V. Banerjee, *Physical Review B* **94**, 094425 (2016).
- [36] M. Anand, J. Carrey, and V. Banerjee, *Journal of Magnetism and Magnetic Materials* **454**, 23 (2018).
- [37] S. Bedanta and W. Kleemann, *Journal of Physics D: Applied Physics* **42**, 013001 (2008).
- [38] C. Haase and U. Nowak, *Physical Review B* **85**, 045435 (2012).
- [39] M. Schabes and A. Aharoni, *IEEE Transactions on Magnetics* **23**, 3882 (1987).
- [40] V. Russier, *Journal of Applied Physics* **89**, 1287 (2001).
- [41] C. C. Dantas and L. A. de Andrade, *Physical Review B* **78**, 024441 (2008).
- [42] J. Carrey, B. Mehdaoui, and M. Respaud, *Journal of Applied Physics* **109**, 083921 (2011).

- [43] E. C. Stoner and E. Wohlfarth, Philosophical Transactions of the Royal Society of London. Series A, Mathematical and Physical Sciences **240**, 599 (1948).
- [44] G. Wysin, available on <https://www.phys.ksu.edu/personal/wysin/notes/demag.pdf> (2012).
- [45] A. García-Arribas, E. Fernández, A. V. Svalov, G. V. Kuryandskaya, A. Barrainkua, D. Navas, and J. M. Barandiaran, The European Physical Journal B **86**, 136 (2013).

a (nm)	$\Theta = D/KV$
10	1.75
12	1.01
16	0.42
20	0.22
30	0.06
40	0.03

TABLE I. Evaluation of the ratio $\Theta = D/KV$ for Fe_3O_4 as a function of interparticle separation a for cubical shaped particle. The lateral dimension of the particle is $l = 10$ nm.

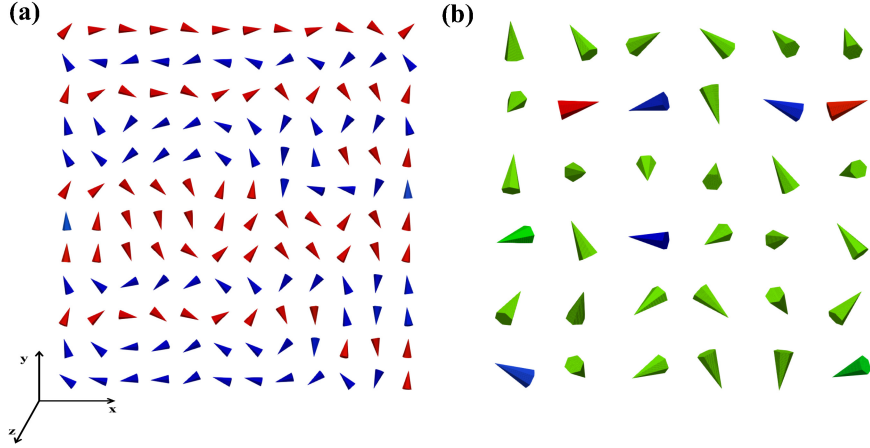


FIG. 1. Typical GS morphologies for: (a) $L_x = L_y = 120$ nm, $a = 10$ nm and $\Theta = 1.75$; (b) $L_x = L_y = 120$ nm, $a = 20$ nm and $\Theta = 0.22$. The magnetic moments are coloured with red colour cone, which has a positive x component, and the magnetic moments with negative x component are coloured blue colour cone. Those with a non-zero z component, and pointing normal to the xy -plane, are indicated with shown with green colour cone. For $\Theta \simeq 0$, moments are randomly oriented, and they also tend to orient normal to the plane of the sample. For $\Theta > 1$, the moments predominantly lie in the xy -plane and exhibit local order.

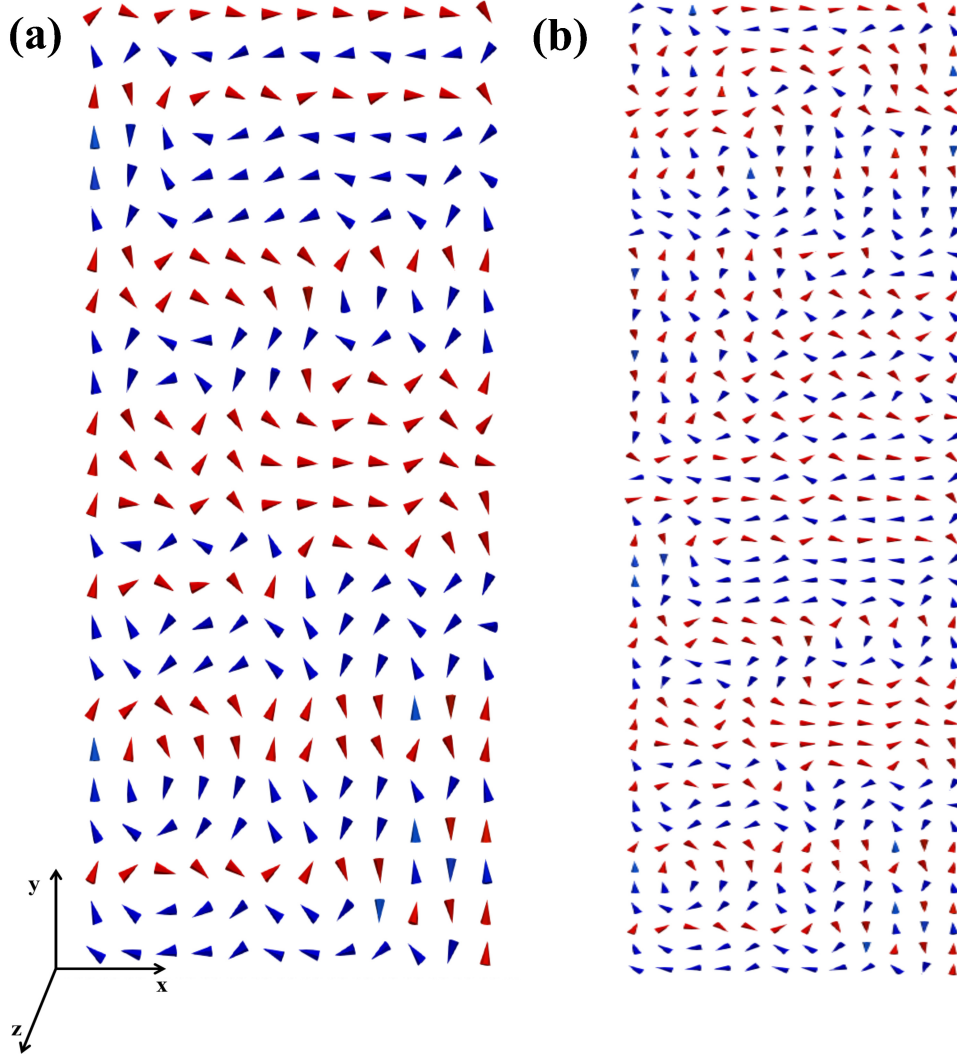


FIG. 2. Typical GS morphologies for strongly interacting MNPs ($a = 10$ nm, $\Theta = 1.75$) as a function of aspect ratio A_r . (a) $L_x = 120$ nm and $A_r = 2$ (b) $L_x = 120$ nm and $A_r = 4$. Due to large dipolar strength, there is an order in the morphology, and they also tend to orient in the plane of the sample. As A_r is increased, magnetic moments also favour chain arrangement along the longer the axis of the sample. The colour coding is the same as described in Fig. (1).

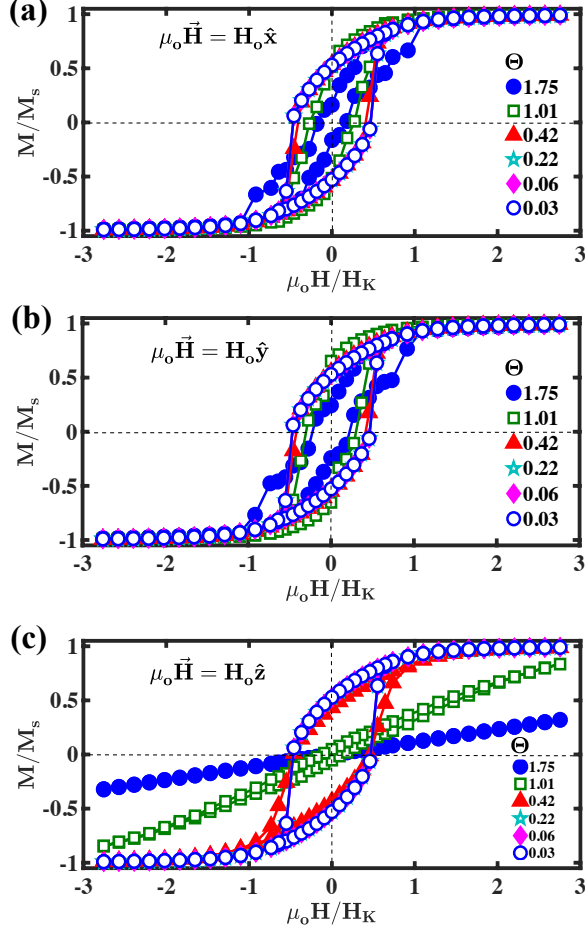


FIG. 3. Magnetic hysteresis behaviour as a function of dipolar interaction strength and direction of the applied field for square sample, i.e., $A_r = 1.0$ ($L_x = L_y = 120$ nm). (a) The external field $\mu_o \vec{H}$ is applied along the x -direction, (b) $\mu_o \vec{H} = H_o \hat{y}$ and (c) $\mu_o \vec{H} = H_o \hat{z}$. The strength of dipolar interaction has been varied from very large value 1.75 to 0.03. When the field is applied in the plane of the sample, coercive field H_c and remanent magnetization decrease with an increase in the strength of the dipolar interaction. When the field is applied is normal to the plane of the sample, H_c and M_r decrease to zero for large dipolar strength. The coercive field $H_c \approx 0.48H_K$ and $M_r \approx 0.5$ are observed for weakly interacting MNPs irrespective of the direction of the applied field as expected (signature of the Stoner-Wohlfarth model).

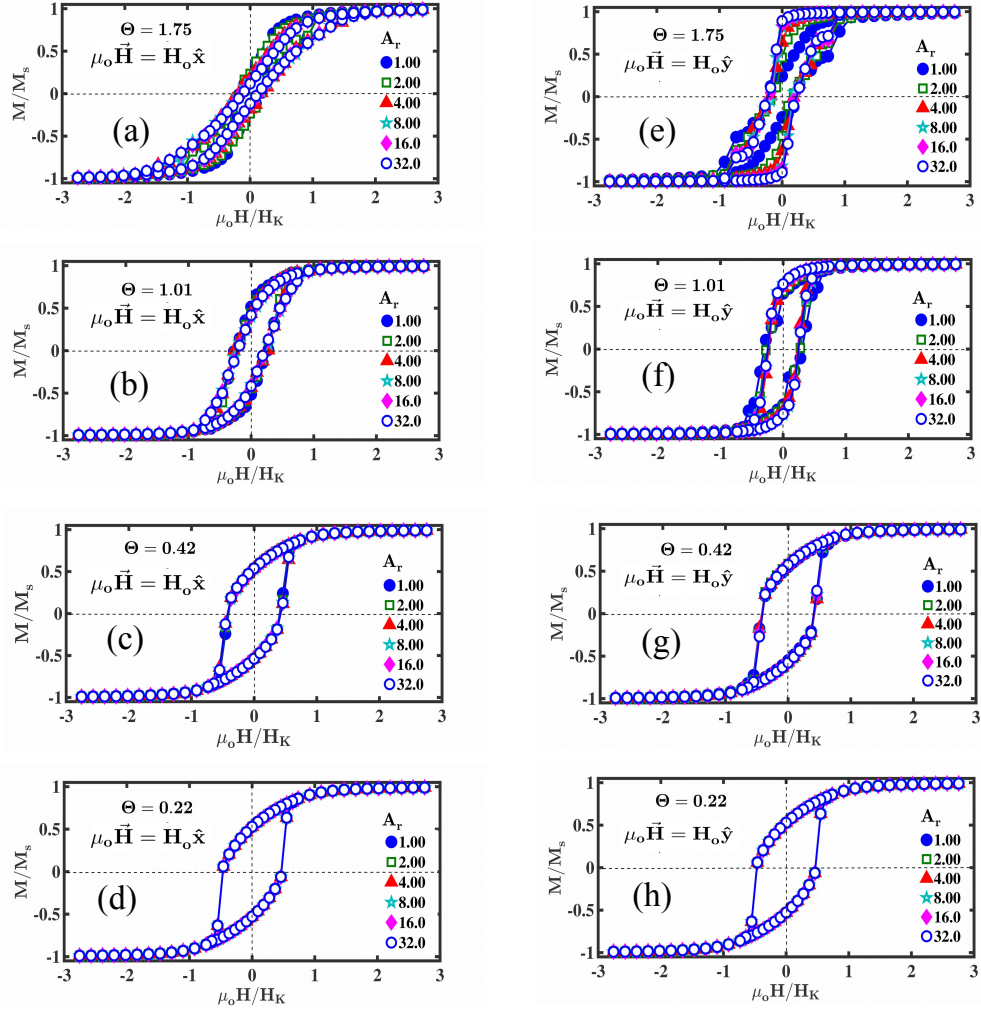


FIG. 4. Dependence of magnetic hysteresis on aspect ratio A_r and dipolar interaction strength Θ when the field is applied in the plane of the sample the sample, i.e., along x -direction [Left Panel: Figure 4(a)-(d)] or y -direction [Right Panel: Figure 4(e)-(h)]. Four values of $\Theta = 1.75, 1.01, 0.42$ and 0.22 have been considered. The aspect ratio A_r is varied from 1.0 to 32.0 in each case. The dipolar interaction decreases the coercive field H_c and M_r . There is a strong dependence of M_r on the shape anisotropy introduced by increasing A_r , M_r reaches to 0.9 when the field is applied along the longer axis of the sample in the presence of strong dipolar interaction. For weak dipolar interaction, i.e., $\Theta = 0.22$, magnetic hysteresis follow the Stoner-Wohlfarth model ($H_c \approx 0.48H_K$ and $M_r \approx 0.5$) irrespective of A_r .

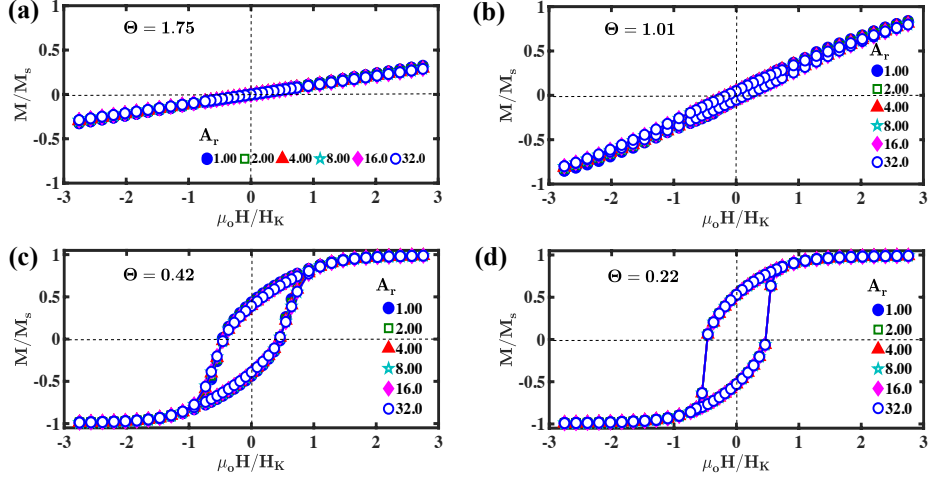


FIG. 5. Magnetic hysteresis as a function of dipolar interaction strength Θ and aspect ratio A_r when the field is applied normal to the plane of the sample $\mu_o \vec{H} = H_o \hat{z}$. Four values of $\Theta = 1.75, 1.01, 0.42$ and 0.22 have been considered. The aspect ratio A_r is varied from 1.0 to 32.0 in each case. For large dipolar interaction strength, the magnetic moments cease to align normal to the sample as a result, non-hysteresis is observed. The coercive field H_c and M_r drop down to zero in this case. For weak dipolar interaction, i.e., $\Theta = 0.22$, magnetic hysteresis follow the Stoner-Wohlfarth model ($H_c \approx 0.48H_K$ and $M_r \approx 0.5$) irrespective of the aspect ratio A_r .

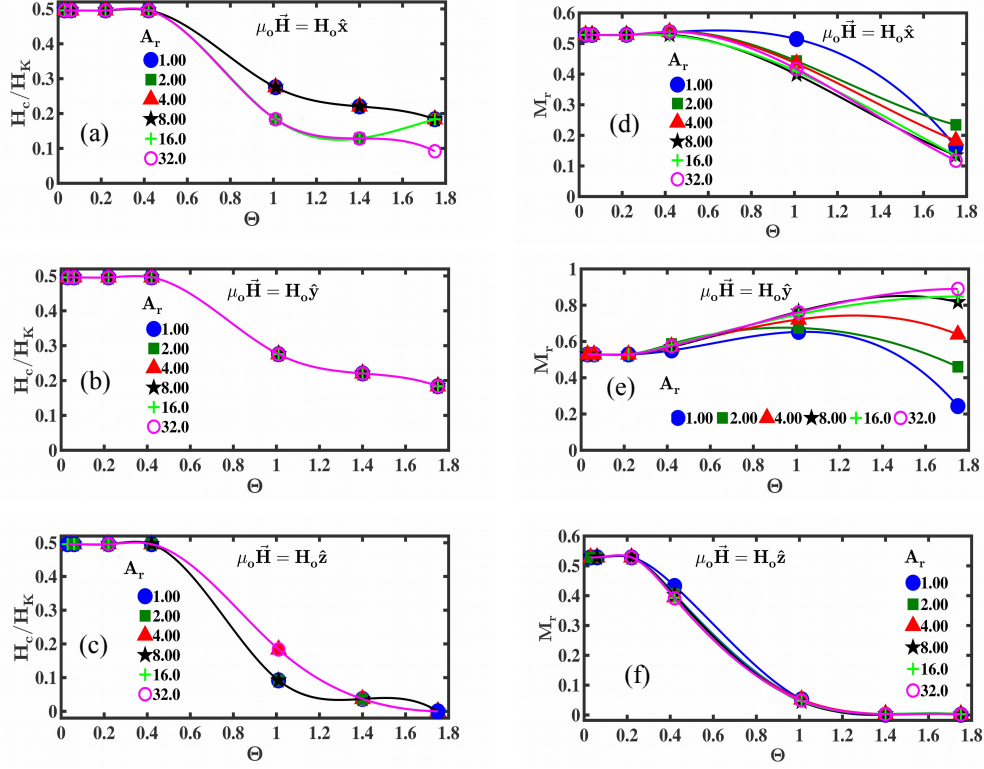


FIG. 6. Coercive field H_c and remanent magnetization M_r variation as a function of dipolar interaction strength Θ , aspect ratio A_r and direction of the applied field. H_c has been scaled by single particle anisotropy field H_K . H_c decreases with an increase in dipolar strength Θ and A_r when the field is applied in the plane of the sample (either along \hat{x} or \hat{y} -axis). H_c drops down to zero when the field is applied normal to the plane of the sample for strongly interacting MNPs. When the field is applied along the x -direction, M_r is decreased with an increase in aspect ratio and dipolar interaction strength Θ . There is a strong shape anisotropy effect is observed when the field is applied along the longer axis of the sample. M_r increases with increase in Θ and A_r , and it reaches to 0.9 with $A_r = 32.0$ and $\Theta = 1.75$. When the external field is applied normal to the plane of the sample $\mu_0 \vec{H} = H_0 \hat{z}$, M_r decreases with increase in A_r and Θ , and it drops down to zero for $\Theta = 1.75$ and $A_r = 32.0$.